Propagating topological transformations in thin immiscible bilayer films

2014 EPL 105 66001

(http://iopscience.iop.org/0295-5075/105/6/66001)

A Letters Journal Exploring the Frontiers of Physics

March 2014

EPL, **105** (2014) 66001
doi: 10.1209/0295-5075/105/66001

www.epljournal.org

Propagating topological transformations in thin immiscible bilayer films

M. G. Hennessy[1], V. M. Burlakov[1], A. Münch[1], B. Wagner[2,3] and A. Goriely[1]

[1] *Mathematical Institute, University of Oxford - Woodstock Road, Oxford, OX2 6GG, UK*
[2] *Department of Mathematics, Technische Universität Berlin - Straße des 17. Juni 136, 10623 Berlin, Germany*
[3] *Weierstrass Institute - Mohrenstraße 39, 10117 Berlin, Germany*

received 11 December 2013; accepted in final form 11 March 2014
published online 28 March 2014

PACS 64.60.My – Metastable phases
PACS 64.75.St – Phase separation and segregation in thin films
PACS 68.05.Cf – Liquid-liquid interface structure: measurements and simulations

Abstract – A physical mechanism for the topological transformation of a two-layer system confined by two substrates is proposed. Initially the two horizontal layers, A and B, are on top of each other, but upon a sufficiently large disturbance, they can rearrange themselves through a spontaneously propagating sectioning to create a sequence of vertical alternating domains ABABAB. This generic topological transformation could be used to control the morphology of fabricated nanocomposites by first creating metastable layered structures and then triggering their transformation. The generality is underscored by formulating conditions for this topological transformation in terms of the interface energies between phases and substrates. The theoretical estimate for the width of the domains is confirmed by simulations of a phase-field model and its thin-film/sharp-interface approximation.

Introduction. – Progress in nanotechnology relies on our ability to design and create regular structures at the smallest scale. This is mostly achieved by self-assembly, *i.e.*, the tendency of molecular/atomic building blocks to organise themselves through simple physical mechanisms [1–3]. In most cases, self-assembly involves first-order phase transformations in the precursor atomic/molecular system following the generic stages of nucleation, growth, and coarsening [4–8]. For instance, key materials for photovoltaics are fabricated via phase separation of multi-component solutions [9–12]. These materials acquire their desired functional properties through their microstructure which is determined by the coarsening stage of phase separation, a difficult process to control [13,14].

Phase separation in confined geometries has been at the focus of intensive research to understand the influence of the conditions at the bounding substrates on the phase-separation kinetics. Several experimental [15–17] and theoretical [18–23] studies have shown that if one of the components of a binary mixture is preferentially attracted to or repelled by a bounding surface, surface-directed spinodal decomposition can occur where composition waves propagate into the bulk with wave vectors that are normal to the surface. These waves can lead to the formation of metastable layered morphologies. Such states can persist for a long time [12,21,24,25] until a large fluctuation or a deliberately introduced perturbation brings the interface between the layers in contact with a substrate since this requires a temporary extension of the interface. The growth rate of the layers often depends on the properties of the system [18,26], *e.g.*, the surface potential; however, studies have found that the early and late stages of growth can be dominated by diffusion and hydrodynamics, respectively [27,28], which is analogous to the coarsening of bulk domains in traditional spinodal decomposition.

In this letter we propose a novel way of fabricating composite nanostructures using controlled switching of phase-separated systems between two distinct metastable states. The initial metastable state consists of a simple bilayer of an A-rich and a B-rich domain sandwiched between two substrates. This bilayer can be created by gradients in the initial composition [25], forced temperature differences across the film [29], or by slowly cooling the system (see text below or [30]). Once this initial structure is created it can be disturbed by generating a single "hole" in one of the layers (see fig. 1(a)). We investigate the conditions under which this initial disturbance triggers a new hole in the opposite layer (fig. 1(b)), hence triggering a cascade of rupturing events (fig. 1(c)) that leads to a system

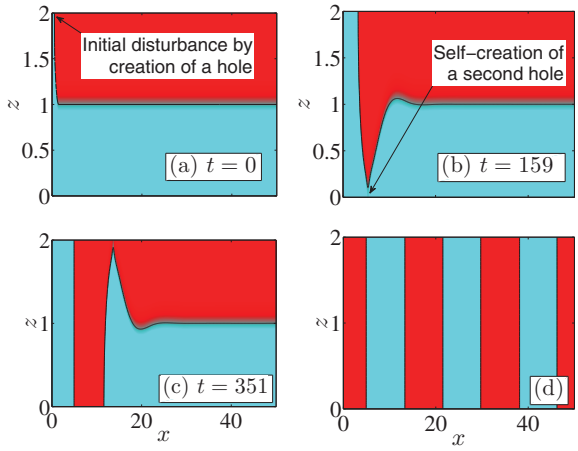

Fig. 1: (Colour on-line) In a geometrically confined phase-field model with coordinate x that extends indefinitely in a direction parallel to two substrates at $z = 0, d$, a topological transformation in a bilayer of two phases is induced by the creation of a single hole (a) in the upper layer. Under the correct conditions, this initial hole can generate a second hole in the lower layer (b). This process repeats itself and triggers a cascade of hole generation (c) resulting in the creation of a periodic array of stripes (The contour line represents $\phi = 0$ in the phase-field model and the system is symmetric about $x = 0$; see text for details).

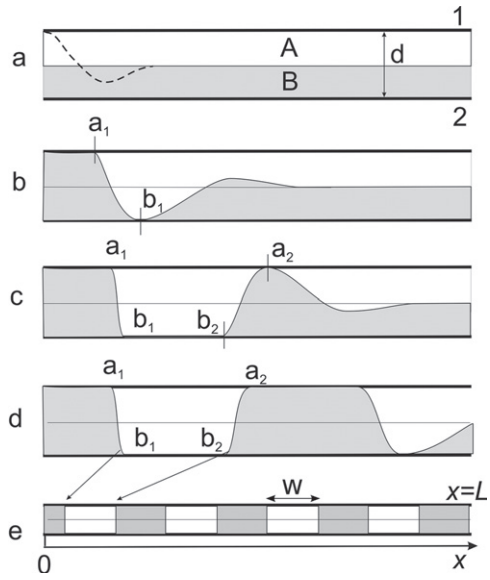

Fig. 2: Configurations of interfaces between immiscible materials A and B during the topological transformation. The domains are symmetric with respect to $x = 0$. Explanations are given in the text.

with alternating A-rich and B-rich trapezoidal "domains" along the substrates (see fig. 1(d)). Note that symmetry is assumed about the vertical axis $x = 0$ in fig. 1, so the disturbance propagates to the left and to the right. We show that this topological transition from two horizontal stripes to an array of vertical stripes is a generic mechanism that can be understood as a consequence of energy reduction and mass conservation. We first give an energy analysis of this process that establishes conditions under which the rupturing cascade occurs and provides estimates for the typical width of the domains. These predictions are checked against simulations of phase-field and thin-film models when the domains are expected to be small and large, respectively.

Energy analysis. – We consider two horizontal layers of equal thickness $d/2$ consisting of immiscible or only partially miscible species A and B. These layers are sandwiched between substrates 1 and 2, with the A-rich phase on top of the B-rich phase (see fig. 2(a)). Next, we disturb the A-B interface so that it touches the upper substrate; see dashed line in fig. 2(a). It may be energetically favourable for phase B to increase the contact area with substrate 1 while simultaneously decreasing the length of the interface with phase A. Due to mass conservation, the trough in the interface will grow and touch substrate 2, see fig. 2(b). At this point, if it is favourable for A to trade a shorter A-B interface length for a wider contact area with substrate 2, the rim will grow as the B phase retracts until it hits substrate 1 (fig. 2(c)), after which the process is repeated, leading to an array of stripes (fig. 2(d), (e)).

We consider a system of finite but large horizontal size L along the x-axis, and consider rupture events for which the A-B interface remains horizontal and flat at $x = L$. To find the conditions for spontaneous propagation of such a topological transformation, we consider the following three stages. First, before initiation, the energy per unit length of the system in fig. 2(a) is $\mathcal{E}_a = (-\gamma_{A1} - \gamma_{B2} + \gamma_{AB})L$, where γ_{ij} denotes the interface energy between phases and substrates i and j, taken to be positive when the interaction is attractive and negative otherwise (γ_{AB} is always positive). We assume that $\gamma_{A1} \geq \gamma_{B1}$, $\gamma_{B2} \geq \gamma_{A2}$ and define the two static contact angles $\cos\theta_1 = (\gamma_{A1} - \gamma_{B1})/\gamma_{AB}$ and $\cos\theta_2 = (\gamma_{B2} - \gamma_{A2})/\gamma_{AB}$.

The second stage corresponds to the moment where phase A first makes contact with substrate 2 (fig. 2(b)). The energy in this configuration is $\mathcal{E}_b = -\gamma_{A1}(L - a_1) - \gamma_{B2}L - \gamma_{B1}a_1 + \gamma_{AB}l^L_{a_1}$ where $l^{x_2}_{x_1}$ denotes the length of the A-B interface between $x = x_1$ and $x = x_2$. The energy difference between the two is

$$\Delta_{ba} = \mathcal{E}_b - \mathcal{E}_a = (\gamma_{A1} - \gamma_{B1})a_1 + \gamma_{AB}(l^L_{a_1} - L). \quad (1)$$

The transition from a to b in fig. 2 reduces energy if $\Delta_{ba} < 0$. Since $L - a_1 < l^L_{a_1} < L - a_1 + 2d$, $\Delta_{ba} < 0$ implies that $2d < a_1(1 - \cos\theta_1)$ which implies both that $a_1 > 2d$ and that the phase B only partially wets the upper substrate, that is, $0 < \theta_1 \leq \pi/2$. Similarly, a necessary condition for the retraction of the AB contact lines at substrate 2 is that A only partially wets substrate 2, *i.e.* the contact angle satisfies $0 < \theta_2 \leq \pi/2$.

The third stage begins when the rim in the B phase touches substrate 1 as in fig. 2(c). The energy in this

stage is $\mathcal{E}_c = -\gamma_{B1}a_1 - \gamma_{A1}(L-a_1) - \gamma_{B2}(b_1-b_2+L) - \gamma_{A2}(b_2-b_1) + \gamma_{AB}(l_{a_1}^{b_1} + l_{b_2}^{L})$. As before, we compute the energy between the two stages

$$\Delta_{cb} = (\gamma_{B2}-\gamma_{A2})(b_2-b_1) + \gamma_{AB}(l_{a_1}^{b_1} + a_1 - b_2), \quad (2)$$

where we have made the assumption that the points a_i, b_i do not move significantly between stages and that the interface profile in stage c between b_2 and L is similar to the interface profile in stage b between a_1 and L up to a horizontal translation, that is $l_{a_1}^{L} = l_{b_2}^{L} + b_2 - b_1$. Then, $\Delta_{cb} < 0$ if both $0 < \theta_2 \leq \pi/2$ and $w_b > 2d$ where $w_b = b_2 - b_1$ is the width of the gap along the lower substrate. The first condition was already assumed (for the retraction of the contact line) and the second condition implies that the width in this transformation must be larger than the thickness of each layer.

Thus, if the system transitions from a to b and therefore $\Delta_{ba} < 0$, then the system can further release energy by passing from configuration b to c by opening the gap width and creating a new hole on substrate 1. Once this happens, the profile from a_2 to L is identical as the initial situation in stage a and the transformation propagates along the interface giving rise to an array of alternating domains. In a similar way one may obtain a merging of sufficiently narrow domains. If one of the vertical stripes is perturbed sufficiently so that it detaches from one of the substrates, it will shrink, thereby increasing its aspect ratio until it either becomes a semicircle or touches a neighbouring A stripe. It is then conceivable that the joining of two stripes may induce further mergers and suggests the possibility of a reverse topological transition. We note that a transition to a bilayer configuration has been observed in experiments [31].

Estimate of stripe width. – Next we estimate the width w of a domain after it has equilibrated (fig. 2(e)). The domains in their equilibrium state are trapezoids and we measure the widths along the centerline between the substrates. Thus, the width can be computed via $w = b_2 - a_1$. We scale all lengths with respect to the thickness of a layer, that is, $d = 2$, and we refer to the profile of the interface in stage b and c as $h_b(x)$ and $h_c(x)$, respectively. Due to mass conservation, $\int_{b_1}^{L} h_b(x)\mathrm{d}x = \int_{b_2}^{L} h_c(x)\mathrm{d}x$. By symmetry, the two profiles h_b and h_c in these intervals can be represented as $h_b(x) = 2 - H(x-a_1)$ and $h_c(x) = H(x-b_2)$ so that

$$\int_{b_1-a_1}^{L-a_1} [2 - H(y)]\mathrm{d}y = \int_{0}^{L-b_2} H(y)\mathrm{d}y \quad (3)$$

To complete the argument, we need an approximation for the profile $H(y)$. We assume that the rim profiles evolve slowly so they are close to equilibrium. The profile has a maximum at $y = \delta = a_2 - b_2$ and a local minimum at $y = \lambda$. We therefore use a piecewise function for H that has nearly constant curvature in the rim and is flat away from it. The two parts are joined smoothly at a point $y = \lambda$ to avoid singularities in the curvature. We have six conditions for the approximation of $H(y)$ of the rim part $y < \lambda$, with two conditions at the contact line $y = 0$, at the maximum, and at $y = \lambda$, namely $H(0) = 0$, $H'(0) = \theta$ (for small contact angles θ), $H(\delta) = 2$, $H'(\delta) = 0$, $H(\lambda) = 1$, $H'(\lambda) = 0$, where δ and λ are unknowns.

These conditions can be satisfied at the lowest order by a cubic polynomial for H. This yields $\delta = 4.62/\theta$, $\lambda = 11.4/\theta$, and fixes the profile to be

$$H(y) = \begin{cases} \theta y - 0.152\,(\theta y)^2 \\ \qquad +0.630\times 10^{-2}\,(\theta y)^3, & \text{if } y \leq \lambda, \\ 1, & \text{if } y > \lambda. \end{cases} \quad (4)$$

Upon evaluating the integrals in (3), L drops out and we obtain $w = 13.2/\theta$.

For contact angles close to $\pi/2$, we choose a different interpolant using an arc-length parameterization S for the non-flat part of the profile such that $S = 0$ is where the approximation for the rim connects to the flat part of the film, and $S = S_1$ and $S = S_2 > S_1$ are the values where the profile has its maximum value for y and the contact line, respectively. We let $x_S = \cos\alpha(S)$, $y_S = \sin\alpha(S)$, where $\alpha(S)$ is a quadratic function in S (a linear function would correspond to the section of a circle and cannot be connected smoothly with the flat part of the film). This function is chosen so that the three conditions $\alpha = \pi$, π, $\theta + \pi$ are satisfied at $S = 0$, S_1 and S_2 respectively. This leaves S_1, S_2 and the integration constants for $x(S)$ and $y(S)$ undetermined, which are fixed by requiring $x(S_2) = 0$, and $y = 1$, 2, 0, at $S = 0$, S_1 and S_2. Using the resulting profile in (3) yields $w = 9.24$ for $\theta = 85°$ and $w = 8.77$ for $\theta = 90°$. For small θ, we recover the previous result and in fact, we find that $13.2 < w\theta < 13.8$ for the entire range of contact angles between 0 and 90°.

Phase-field model. – We use a phase-field model to show that the formation of a bilayer is possible by slowly cooling the system, and for constant temperatures, we compare numerical simulations to the theoretical results from the previous section. We assume purely diffusive transport and describe the kinetics by a two-dimensional Cahn-Hilliard model [32–36] for the order parameter $\phi(x, z, t)$ on $0 < z < d = 2$,

$$\phi_t = \Delta\mu, \quad \mu = f'(\phi) - \varepsilon^2\Delta\phi, \quad (5)$$

where Δ is the Laplacian operator, $f(\phi) = \frac{1}{2}\left(\phi^2 - \chi(t)\right)^2$ is the homogeneous contribution to the bulk free energy and μ is the chemical potential of the mixture. Here, the function $\chi(t)$ is a measure of the temperature relative to the bulk critical temperature and it satisfies $0 < \chi(t) < 1$ for all time, where $\chi = 0$ corresponds to the critical temperature and $\chi = 1$ is some temperature below this value. We assume the mixture to be symmetric, $f(\phi) = f(-\phi)$, and ϕ has been scaled so that when the temperature is constant with $\chi \equiv 1$, the minima of f are located at $\phi = 1$

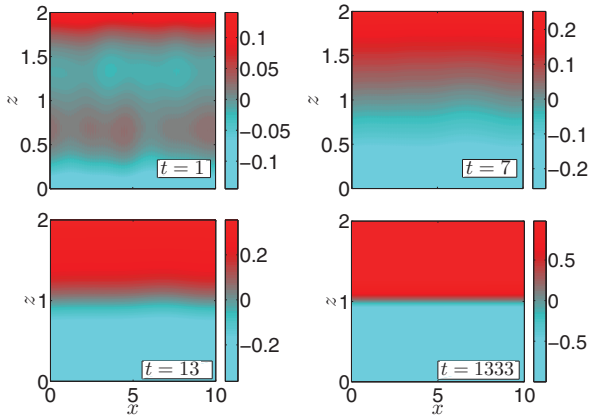

Fig. 3: (Colour on-line) Phase-field simulations showing that a bilayer can be produced from a noisy initial condition if the temperature of the system is slowly cooled from the critical value and the substrates have a small amount of surface energy. See text for details.

and -1 for the equilibrated homogeneous A-rich and B-rich phase, respectively. The parameter ε, $0 < \varepsilon \ll 1$, determines the width of the diffuse A-B interface compared to the typical thickness of the B-layer. In a lattice model derivation, ε depends on the effective range of the interactions between the molecules and the temperature [32,36]. The model is valid close, but not too close, to the critical point [36]. At the boundaries $z = 0$, d, we impose no flux and include the effect of surface energies,

$$\mu_z = 0, \qquad \varepsilon\phi_z = \beta(1-\phi^2). \tag{6}$$

The second condition corresponds to antisymmetric substrates with a surface energy density $f_s(\phi) = \beta(\phi - \phi^3/3)$ at the bottom and $-f_s(\phi)$ at the top surface. We have also chosen f_s so that at constant temperatures, *i.e.*, $\chi \equiv 1$, we have $\mathrm{d}f_s/\mathrm{d}\phi = 0$ for $\phi = \pm 1$, which facilitates the evaluation of the static contact angle [37,38], since it avoids contributions from surface boundary layers; see [39].

Solutions to the phase-field model (5) are computed numerically for $\varepsilon = 0.127$ with a scheme that uses a finite-difference discretisation in time and spectral methods for spatial derivatives. We take $d = 2$ and assume x is periodic on the domain $[-L, L]$. Moreover, in all calculations, symmetry is assumed with respect to $x = 0$.

Figure 3 shows that cooling the system results in a bilayer configuration. The initial condition was chosen to be uniformly distributed random numbers between ± 0.2; the temperature was varied according to $\chi(t) = 1 - \exp(-t/\tau_c)$, where $\tau_c = 133$; the surface energy of the substrates was set to $\beta = 0.063$; and the domain was truncated at $L = 10$. For early times when the temperature of the system is just below criticality and $\chi(t) \ll 1$, the two materials are strongly attracted to their preferred wall and this leads to the formation of compositional boundary layers. Although small fluctuations to a homogeneous state are amplified below the critical temperature, a linear stability analysis with $\chi(t)$ held constant indicates the maximal amplification rate is $(\chi/\varepsilon)^2$ which is very small for $\chi < \varepsilon$. As the temperature is further decreased, these boundary layers grow in thickness and induce a layered morphology. By cooling at a slow rate the system evolves in a quasi-stationary manner; that is, at each moment in time the system is close to being in its instantaneous steady state if $\chi(t)$ was frozen. These steady states are linearly stable so small perturbations to them, *e.g.*, from thermal fluctuations, are not expected to be amplified. The complete mathematical details of the cooling process are presented in [40].

For the remainder of the letter, the temperature is held constant with $\chi \equiv 1$. Figure 1(a)–(d) shows an example of the propagating topological transformation occurring in the phase-field model for $L = 50$ and $\theta = 90^\circ$ (or $\beta = 0$); in this case the substrates do not interact with either species. At time $t = 0$ the bilayer is disturbed in such a way that the B-rich phase has already penetrated the upper layer up to the substrate. A cascade of rupturing events unfolds as predicted by the energy analysis and shown in panel (b) and (d), leading to a series domains with straight interfaces meeting the substrates at an angle of $\theta = 90^\circ$. The widths of the first five domains at the centerline are, in order from left to right, 4.6, 8.0, 8.2, 8.4, 8.4, in good agreement with the estimate $8.4 < w < 8.8$ derived in the previous section.

As expected, the total free energy

$$F = \int_0^L \int_0^d f_b(\phi(x,z))\mathrm{d}z + \varepsilon\, f_s(\phi(x,z))|_{z=0}^{d}\,\mathrm{d}x,$$

with $f_b(\phi) = f(\phi) + (\varepsilon^2/2)|\nabla\phi|^2$, decreases monotonically (not shown) with reduction of the A-B interface. A rapid decrease in the free energy occurs when the ridge of the retracting layer comes into contact with a substrate during the final stages of each rupturing event.

Thin-film model. – In the limit of thin diffuse layer at the interface between A and B, the phase-field model tends to the Mullins-Sekerka sharp interface model [41] and an equilibrium contact angle [37,38] $\theta = \cos^{-1}\beta$. For an interface $z = h(x,t)$ separating layers of A and B, this model can be written explicitly as

$$\Delta\mu_1 = 0, \quad \text{on } 0 < z < h \text{ and } h < z < d, \tag{7a}$$

$$\mu_1 = \frac{2}{3}\frac{h_{xx}}{(1+h_x^2)^{3/2}}, \quad \text{at } z = h, \tag{7b}$$

$$h_t = \frac{\varepsilon}{2}\left([\partial_x\mu_1]_-^+ h_x - [\partial_z\mu_1]_-^+\right), \quad \text{at } z = h, \tag{7c}$$

$$\partial_z\mu_1 = 0, \qquad \text{at } z = 0, d. \tag{7d}$$

Notice that $[\cdot]_-^+$ is the jump across the interface. Integrating (7a) with respect to z and using the boundary conditions (7c) and (7d) yields a conservation equation

$$h_t + q_x = 0, \qquad q = \frac{\varepsilon}{2}\int_0^d \mu_{1,x}\,\mathrm{d}z, \tag{7e}$$

which is supplemented with boundary conditions at the contact line $x = s(t)$ given by

$$h = 0, \qquad h_x = \tan\theta, \qquad q = 0. \tag{7f}$$

These represent the presence of a contact line, a static contact angle θ, and no flux, respectively. In the far field the interface corresponds to that of the undisturbed bilayer, hence we impose $h \to 1$ as $x \to \infty$.

When the contact angle is small, $\theta \ll 1$, simplifications to this model are possible by writing

$$x = \theta^{-1}\tilde{x}, \quad t = \frac{3}{\varepsilon d\theta^4}\tilde{t}, \quad \mu_1 = \theta^2\tilde{\mu}, \quad q = \frac{\varepsilon d\theta^3}{3}\tilde{q} \tag{8}$$

in (7) and then taking the limit $\theta \to 0$. The resulting system for $\tilde{\mu}$ can be solved and an explicit thin-film equation for the evolving interface can be obtained. Written in terms of the original variables, this equation is given by

$$h_t + q_x = 0, \qquad q = \frac{\varepsilon d}{3}h_{xxx}, \tag{9a}$$

$$\lim_{x\to\infty} h = 1, \tag{9b}$$

$$h = 0, \qquad h_x = \theta, \qquad q = 0 \quad \text{at } x = s(t). \tag{9c}$$

This dimension-reduced model not only facilitates greatly large-scale numerical simulations, but the existing large body of literature on these types of thin-film equations can now be used to assess the dynamics, morphology and stability properties of the interfaces. Moreover, the system in (9) can be put into parameter-free form using the scalings in (8). Thus, all of the dynamics that occur at small contact angles can be extracted from a single simulation of the thin-film equation.

The results for $L \gg 100$ are shown in fig. 4, starting from a hole in the A-rich phase near the origin. The first domain is determined by this initial condition and has a width of $7.14/\theta$, while for the second and all subsequent domain the width has converged to the limiting value $13.0/\theta$, which is very close to the estimate of $13.2/\theta$ obtained in the previous section for small contact angle (as found for thin films). These domains are trapezoidal due to the equilibrium contact angle being less than 90° and the largest horizontal edge is always in contact with the preferred substrate. As the contact angle increases to 90° the domains become rectangular as shown in fig. 1.

The geometrical aspects of the domains that emerge in simulations of the phase-field and thin-film models are in good agreement. When $\theta = 50°$ and $\varepsilon = 0.2$, the relative difference in the width of the second domain is roughly 12% and for subsequent domains it is less than 10%. However, the times at which new contact lines are created differ significantly in the two models. The first topological transformation in the thin-film model occurs when $\tilde{t} = 118$ (see fig. 4) whereas in the phase-field model with $\theta = 20°$ and $\varepsilon = 0.2$ this time is $\tilde{t} = 43$. Thus, the rupturing process is accelerated in the phase-field model and this seems to be due to wall effects that are not included in the thin-film equation. Further details of the comparison are presented in [40].

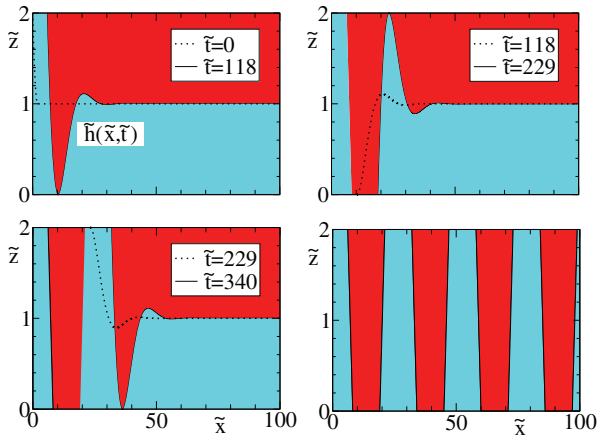

Fig. 4: (Colour on-line) Numerical simulations using the thin-film approximation (9a), starting from an initial hole near $x = 0$ with the B-rich phase (blue, light) penetrating the A-rich phase (red, dark). Shown is the situation after the first, second, third and many rupture events, respectively. Results are given in terms of the rescaled variables $\tilde{x} = \theta x$ and $\tilde{t} = (\varepsilon d\theta^4/3)t$.

The time scale on which a 1:1 bilayer undergoes a complete transformation to a laterally separated configuration can be estimated as $Nt_{\rm rup}$, where N is the number of domains and $t_{\rm rup}$ is the time between successive ruptures. When the contact angle is small these quantities are given by

$$N \simeq \frac{L_d}{W_d} \simeq 0.15\frac{\theta L_d}{H_d}, \quad t_{\rm rup} = \frac{3}{8}\frac{H_d^3}{Da\theta^4}\frac{T/T_c}{\sqrt{1-T/T_c}}\tilde{t}_{\rm rup},$$

where L_d and H_d are the dimensional length and height of the bilayer, respectively, and W_d is the width of each domain. Furthermore, a is a molecular interaction length, D is the diffusion coefficient, T and T_c are the temperature and critical temperature, respectively, and $\tilde{t}_{\rm rup}$ is the non-dimensional rupture time computed via simulation. Using the thin-film model we find that $\tilde{t}_{\rm rup} = 111$; see fig. 4. The highly nonlinear dependence of $t_{\rm rup}$ on the bilayer thickness and the contact angle means even small changes in these values can largely affect the time it takes for a single rupture to occur. The temperature also plays an important role in setting the time scale between ruptures with $t_{\rm rup}$ increasing as the critical point is reached. For cooler temperatures the rupture process becomes more rapid.

We can explore ratios of the A-layer to B-layer thickness that are larger than 1:1 by using values of $d > 2$. The resulting vertical domains have relative widths which preserve the ratio $(d-1)$:1 and are both wider than for $d = 2$. The minimum immediately following the rim at a receding contact line decreases as the rim grows, and if $d > 7.96$, it hits the lower substrate before the peak of the rim reaches the upper substrate. As a result, the rim detaches from the remaining film [42]. The resulting pattern therefore typically equilibrates into a string

of B-rich droplets embedded within the A-rich majority phase.

Conclusion. – In this study we describe the topological transformation of two immiscible/partially miscible adjacent horizontal layers confined between two substrates. This transformation suggests a mechanism for self-patterning composite materials via rapid switching from one metastable state to another. Our analysis predicts the dependence of the process and the size of the structures on the thicknesses of the layers and the interfacial energies as well as the surface energies of the confinement.

The scenario we study here is two dimensional, or planar symmetric. Deviations from the two-dimensional situation arise if the initial rupture is pointlike to begin with, favouring an axisymmetric evolution. The cross-section evolves in a similar pattern as in the planar symmetric case, except that the width of the domains is expected to change with the distance from the original rupture event. We also note that the deviations from the planar symmetry can be suppressed or altered by two-dimensional confinement, for example by conducting experiments in cylindrical pores.

* * *

This publication is based in part upon work supported by The James Martin School (VMB, AG) and Award No. KUK-C1-013-04, made by KAUST. AG is a Wolfson/Royal Society Merit Award Holder and acknowledges support from a Reintegration Grant under EC Framework VII. BW gratefully acknowledges the support by the Federal Ministry of Education (BMBF) and the state government of Berlin (SENBWF) in the framework of the program "Spitzenforschung und Innovation in den Neuen Ländern" (Grant No. 03IS2151) and the hospitality of OCCAM.

REFERENCES

[1] Ozin G. A., Hou K., Lotsch B. V., Cademartiri L., Puzzo D. P., Scotognella F., Ghadimi A. and Thomson J., *Mater. Today*, **12**, issue No. 5 (2009) 12.
[2] Mann S., *Nat. Mater.*, **8** (2009) 781.
[3] Ariga K., Hill J. P., Lee M. V., Vinu A., Charvet R. and Acharya S., *Sci. Technol. Adv. Mater.*, **9** (2008) 014109.
[4] Moriarty P., Taylor M. D. R. and Brust M., *Phys. Rev. Lett.*, **89** (2002) 248303.
[5] Otero R., Schöck M., Molina L. M., Lægsgaard E., Stensgaard I., Hammer B. and Besenbacher F., *Angew. Chem., Int. Ed.*, **44** (2005) 2270.
[6] Shevchenko E. V., Talapin D. V., Kotov N. A., O'Brien S. and Murray C. B., *Nature*, **439** (2006) 55.
[7] Bishop K. J. M., Wilmer C. E., Soh S. and Grzybowski B. A., *Small*, **5** (2009) 1600.
[8] Weber U. K., Burlakov V. M., Perdigão L. M. A., Fawcett R. H. J., Beton P. H., Champness N. R., Jefferson J. H., Briggs G. A. D. and Pettifor D. G., *Phys. Rev. Lett.*, **100** (2008) 156101.
[9] Mayer A. C., Scully S. R., Hardin B. E., Rowell M. W. and McGehee M. D., *Mater. Today*, **10**, issue No. 11 (2007) 28.
[10] Thompson B. C. and Fréchet J. M. J., *Angew. Chem., Int. Ed.*, **47** (2008) 58.
[11] Dunbar A. D. F., Mokarian-Tabari P., Parnell A. J., Martin S. J., Skoda M. W. A. and Jones R. A. L., *Eur. Phys. J. E*, **31** (2010) 369.
[12] Coveney S. and Clarke N., *Phys. Rev. Lett.*, **111** (2013) 125702.
[13] Chirvase D., Parisi J., Hummelen J. C. and Dyakonov V., *Nanotechnology*, **15** (2004) 1317.
[14] Brabec C. J., Heeney M., McCulloch I. and Nelson J., *Chem. Soc. Rev.*, **40** (2011) 1185.
[15] Jones R. A. L., Norton L. J., Kramer E. J., Bates F. S. and Wiltzius P., *Phys. Rev. Lett.*, **66** (1991) 1326.
[16] Geoghegan M. and Krausch G., *Prog. Polym. Sci.*, **28** (2003) 261.
[17] Krausch G., *Mater. Sci. Eng.: R: Rep.*, **14** (1995) v.
[18] Puri S. and Binder K., *Phys. Rev. A*, **46** (1992) R4487.
[19] Binder K., *J. Non-Equilib. Thermodyn.*, **23** (1998) 1.
[20] Binder K., Das S. K. and Horbach J., *Mod. Phys. Lett. B*, **23** (2009) 549.
[21] Binder K., Puri S., Das S. K. and Horbach J., *J. Stat. Phys.*, **138** (2010) 51.
[22] Puri S., *J. Phys.: Condens. Matter*, **17** (2005) R101.
[23] Puri S. and Frisch H. L., *J. Phys.: Condens. Matter*, **9** (1997) 2109.
[24] Das S. K., Puri S., Horbach J. and Binder K., *Phys. Rev. E*, **72** (2005) 061603.
[25] Jaiswal P. K., Binder K. and Puri S., *J. Chem. Phys.*, **137** (2012) 064704.
[26] Yan L.-T. and Xie X.-M., *J. Chem. Phys.*, **126** (2007) 064908.
[27] Jaiswal P. K., Puri S. and Das S. K., *EPL*, **97** (2012) 16005.
[28] Krishnan R., Jaiswal P. K. and Puri S., *J. Chem. Phys.*, **139** (2013) 174705.
[29] Jaiswal P. K., Puri S. and Binder K., *EPL*, **103** (2013) 66003.
[30] Ball R. C. and Essery R. L. H., *J. Phys.: Condens. Matter*, **2** (1990) 10303.
[31] Adams C. D., Atzmon M., Cheng Y. T. and Srolovitz D. J., *Appl. Phys. Lett.*, **59** (1991) 2535.
[32] Cahn J. W. and Hilliard J. E., *J. Chem. Phys.*, **28** (1958) 258.
[33] Cahn J. W., *Acta Metall. Mater.*, **9** (1961) 795.
[34] Vladimirova N., *Phys. Rev. E*, **58** (1998) 7691.
[35] Molin D. and Mauri R., *Phys. Fluids*, **19** (2007) 074102.
[36] Binder K., *Acta Polym.*, **46** (1995) 204.
[37] Cahn J. W., *J. Chem. Phys.*, **66** (1977) 3667.
[38] Modica L., *Ann. Inst. Henri Poincaré-Anal.*, **4** (1987) 487.
[39] Xu X. and Wang X., *SIAM J. Appl. Math.*, **71** (2011) 1753.
[40] Hennessy M. G., Burlakov V. M., Goriely A., Münch A. and Wagner B., *Controlled topological transitions in thin film phase separation*, preprint arXiv:1402.6890 (2014).
[41] Pego R. L., *Proc. R. Soc. A*, **422** (1989) 261.
[42] Wong H., Voorhees P., Miksis M. and Davis S., *Acta Mater.*, **48** (2000) 1719.